Imaging individual mRNA molecules using multiple singly labeled probes

Arjun Raj[1], Patrick van den Bogaard[2], Scott A Rifkin[1], Alexander van Oudenaarden[1] & Sanjay Tyagi[2]

We describe a method for imaging individual mRNA molecules in fixed cells by probing each mRNA species with 48 or more short, singly labeled oligonucleotide probes. This makes each mRNA molecule visible as a computationally identifiable fluorescent spot by fluorescence microscopy. We demonstrate simultaneous detection of three mRNA species in single cells and mRNA detection in yeast, nematodes, fruit fly wing discs, and mammalian cell lines and neurons.

As it is becoming increasingly apparent that gene expression in individual cells deviates substantially from the average behavior of cell populations[1], new methods that provide accurate integer counts of mRNA copy numbers in individual cells are needed. Ideally, such methods should also reveal the intracellular locations of the mRNAs, as mRNA localization is often used by cells to spatially restrict the activity of proteins[2]. One candidate for such a method is *in situ* hybridization followed by microscopic analysis[3,4]. A conventional practice is to link probes to enzymes that catalyze chromogenic or fluorogenic reactions[5]. However, because the products of these reactions are small molecules or precipitates that diffuse away from the probe, the location of the target molecule is not precisely determined. Conversely, probes labeled directly with a few fluorophores maintain spatial resolution, but the sensitivity that can be achieved is relatively poor.

To circumvent these problems, a variant of fluorescence *in situ* hybridization (FISH) procedure has been developed that is sensitive enough to detect single mRNA molecules[6]. In this procedure, 5 oligonucleotide probes, each about 50 nucleotides long and labeled with 5 fluorophore moieties, are hybridized to each mRNA target, which then becomes visible as a diffraction-limited fluorescent spot. Although these probes have been used successfully[7], the system has not been widely adopted. One reason for this is difficulty in synthesizing and purifying heavily labeled oligonucleotides: the amine groups used for coupling fluorophores to the probe are prone to loss, and it is hard to purify fully coupled probes from partially coupled ones[8]. Also, when some fluorophores are present in multiple copies on the same oligonucleotide, they interact with each other, altering the hybridization characteristics of the oligonucleotides and resulting in severe self-quenching[9].

Another issue with the use of small numbers of heavily labeled probes is that the signals are more prone to variability. For instance, when using 5 fluorescent probes targeted to a single mRNA, the researchers had estimated that the majority of the fluorescent spots observed have intensities corresponding to the presence of only 1 or 2 probes[6]. This makes it difficult to unambiguously identify all the fluorescent spots as mRNA molecules as it is impossible to determine whether the detection of an individual probe arises from legitimate binding to the target mRNA or from nonspecific binding.

To address these issues, we reasoned that by taking advantage of the high throughput of 96-position DNA synthesizers, one could synthesize a large number of probes and reliably label them with a single fluorophore moiety at their 3′ termini to detect individual mRNA molecules. We constructed a doxycycline-controlled gene

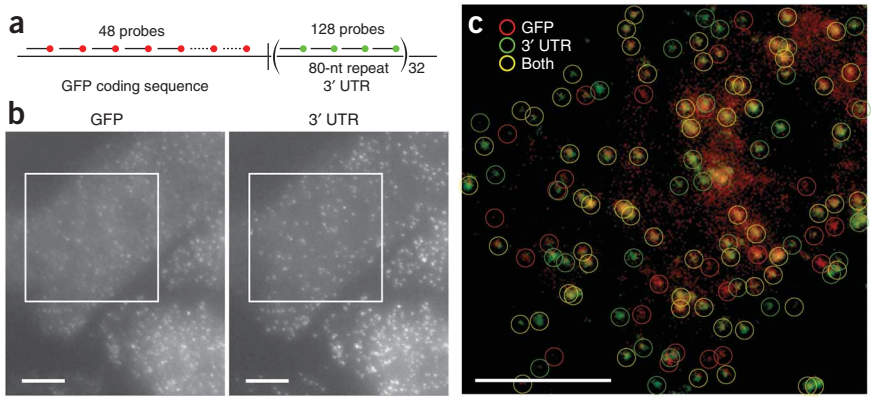

Figure 1 | Simultaneous detection of a unique sequence and a repeated sequence in individual mRNA molecules. (**a**) Schematic of the construct used. The 48 probes used to detect the GFP coding sequence were labeled with Alexa 594, and the four different probes used to detect the tandem repeat in the 3′ UTR were labeled with TMR. (**b**) Maximum intensity merges of a pair of *z*-image stacks of fluorescent images of CHO cells taken in the Alexa 594 channel (left) and the TMR channel (right). (**c**) False-color merge of the boxed regions in **b**, with circles representing computationally identified mRNA particles. Scale bars, 5 μm.

[1]Department of Physics, Massachusetts Institute of Technology, 77 Massachusetts Avenue, Cambridge, Massachusetts 02139, USA. [2]Public Health Research Institute Center, New Jersey Medical School, University of Medicine and Dentistry of New Jersey, 225 Warren Street, Newark, New Jersey 07103, USA. Correspondence should be addressed to A.R. (arjunraj@mit.edu) or S.T. (tyagisa@umdnj.edu).

RECEIVED 25 JUNE; ACCEPTED 25 AUGUST; PUBLISHED ONLINE 21 SEPTEMBER 2008; DOI:10.1038/NMETH.1253

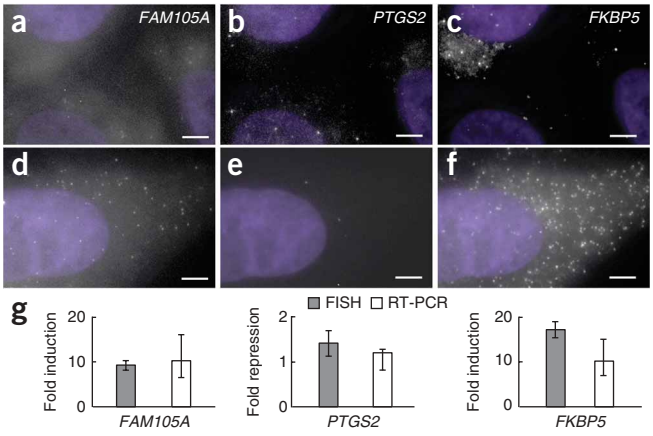

Figure 2 | Simultaneous imaging of three different mRNAs in mammalian cells. (**a–f**) Images showing fluorescent spots corresponding to *FAM105A*, *PTGS2* and *FKBP5* mRNAs in the same set of A549 cells not treated with dexamethasone (**a–c**) and in cells treated for 8 h with 24 nM dexamethasone (**d–f**). (**g**) Fold change in expression for all three genes as measured by FISH and real-time RT-PCR; error bars represent standard errors of measurements (see **Supplementary Methods**). All images are maximum merges of a *z*-stack of fluorescence images spanning the extent of the cells with nuclear 4,6-diamidino-2-phenylindole (DAPI) counterstaining in purple. Scale bars, 5 μm.

that produced an mRNA encoding GFP and contained 32 tandemly repeated 80-nucleotide-long sequences in its 3′ untranslated region (UTR); we then stably integrated this engineered gene into the genome of a Chinese hamster ovary cell line (**Fig. 1a**). Previously, we have shown that fluorescent probes targeted to tandemly repeated copies of probe-binding sequence results in FISH signals corresponding to individual molecules using a variety of methods, including a demonstration that the number of fluorescent spots per cell was about the same as the number of mRNA per cell, as measured by quantitative real-time reverse-transcriptase (RT)-PCR[10,11]. Here we targeted the coding region of the *GFP* mRNA with 48 different oligonucleotides labeled with Alexa 594 fluorophores and targeted each repeat sequence in the 3′ UTR with 4 oligonucleotides labeled with tetramethylrhodamine (TMR).

After hybridization, we imaged the cells with a pair of filter sets that could clearly distinguish between the two fluorophores. We found many 'particles' with a diameter of about 0.25 μm that appeared in both the TMR and Alexa 594 channels (**Fig. 1b**). The particles were identified computationally using an image processing program (**Supplementary Fig. 1**, **Supplementary Methods** and **Supplementary Software** online) that categorizes particles as being labeled with either the GFP-coding-sequence probes (TMR), the UTR-specific probes (Alexa-594) or both (**Fig. 1c**). Upon identifying and localizing particles in four fields of view similar to the ones shown in **Figure 1c**, we counted a total of 599 particles corresponding to GFP coding sequence–specific probes and 565 particles corresponding to the UTR-specific probes. Of these particles, 85% of the 'UTR particles' localized with the 'GFP particles', whereas 81% of the GFP particles colocalized with the UTR particles. The high degree of colocalization between particles detected by the previously established tandem-repeat detection method[10] and the particles detected via simultaneous probing with 48 different singly labeled oligonucleotides demonstrates the validity of using multiple single-labeled probes for the detection of endogenous transcripts. The fraction of particles that did not colocalize likely corresponded to mRNA molecules that lost either their coding sequence or their 3′ UTR via the natural processes of mRNA degradation. An analysis of fluorescence intensity of the colocalized spots showed that the spot intensities displayed a unimodal distribution (**Supplementary Fig. 2** online), arguing that the particles detected were individual molecules[10].

We also explored how the signal intensity varied with the number of probes by performing FISH using either the first 12, 24, or 36 probes or all 48 probes in our set. For this particular target mRNA, we found that particles could be detected with fewer probes, albeit with decreased intensity (**Supplementary Fig. 3a** online). However, our automatic spot-detection algorithm performed particularly well with 48 probes, detecting the same number of spots over a broad range of thresholds (**Supplementary Fig. 3b**). The number of probes required for robust signal is likely to depend on the target sequence, though, as accessibility to probes depends on the secondary structure in the RNA. Our method was at least as sensitive as the FISH-based method[6] described above (**Supplementary Fig. 4** online).

A potential use of our method is to simultaneously detect single molecules of multiple mRNAs in individual cells. To detect three different mRNAs at the same time, we designed probes specific for mRNAs encoding *FKBP5*, *PTGS2* and *FAM105A* in the human carcinoma cell line A549. We coupled these probes to the spectrally distinct fluorophores Cy5, Alexa 594 and TMR, respectively. Upon performing FISH with all three probes simultaneously, individual spots were visible in the three different fluorescence channels (**Fig. 2a–f**). The spots corresponding to different mRNAs did not overlap with each other. An intensity analysis showed that fluorescent spots did not bleed through into other channels (**Supplementary Fig. 5** online) and the use of an oxygen-scavenging mounting buffer ensured the stability of all fluorophores during the acquisition of image stacks (**Supplementary Fig. 6** online).

To demonstrate that our method of mRNA detection was specific and quantitative, we added to the growth medium a cell-permeant glucocorticoid, dexamethasone, which upregulates expression of *FKBP5* and *FAM105A*, and mildly downregulates expression of *PTGS2* in this cell line[12]. The mean number of *FKBP5* and *FAM105A* mRNAs measured by combining FISH with our spot-detection algorithm increased whereas the mean number of *PTGS2* mRNAs decreased (**Fig. 2a–f**). The values we obtained corresponded well to RT-PCR measurements of the fold induction and repression of these genes performed on the same samples, demonstrating that the fluorescent spots are the appropriate mRNAs and that we detected a majority of the mRNA molecules (**Fig. 2g**). This also demonstrated the effectiveness of our spot detection algorithm for accurate gene-expression quantification.

Our method also captured spatial information about the location of the mRNAs detected, a particularly important feature for studying development, in which mRNAs often display spatial patterning. We tested our method for efficacy in two commonly studied developmental systems: the nematode, *Caenorhabditis elegans*, and the fruit fly, *Drosophila melanogaster*. In the nematode, we constructed probes to detect mRNA molecules transcribed from the gene *elt-2*, a transcription factor that is expressed only in the nematode gut and only after the embryo has developed to the

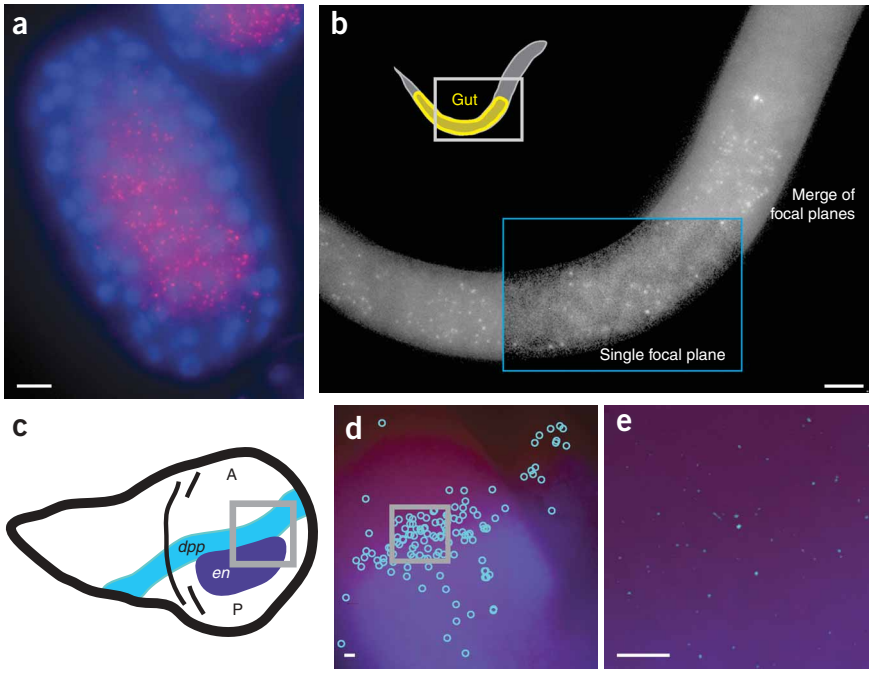

Figure 3 | Imaging localized mRNAs in *C. elegans* and *D. melanogaster*. (**a**) *elt-2* mRNA molecules (magenta) in an early stage *C. elegans* embryo (~100 cell stage); the nuclei were counterstained with DAPI (blue). (**b**) *elt-2* mRNA molecules in a *C. elegans* L1 larva. A single focal plane is shown in the boxed region, in which the intestinal track is visible. (**c**) A schematic of *dpp* and engrailed (*en*) expression in the imaginal wing discs of third instar *D. melanogaster* larvae. (**d**) Image showing the locations of the computationally identified *dpp* mRNA molecules (light blue circles) and Engrailed expression detected by immunofluorescence (dark blue). (**e**) Magnification of the boxed region in **d** showing enhanced *dpp* mRNA molecule signals (light blue) and Engrailed protein expression detected by immunofluorescence (dark blue). All images except the boxed portion in **b** are maximum merges of a *z*-stack of fluorescence images. Scale bars, 5 μm.

45-cell stage[13]. After hybridization of the probe set to both embryos and larvae, we found that *elt-2* mRNA molecules were present only in the gut region (**Fig. 3a**) of both the embryos and the larvae (**Fig. 3b**). Consistent with the known timing of the onset of expression[13], we only detected *elt-2* mRNAs in the gut of embryos older than the 45-cell stage.

In the fruit fly, one of the most well-studied examples of the localization of gene expression occurs in wing imaginal disc development[14]. The wing discs of fruit fly larvae display a remarkable set of gene expression patterns, one of which is the formation of a stripe of expression of the gene *dpp* in response to gradients of the morphogenic proteins Hedgehog and Engrailed[14] (**Fig. 3c**). To check whether this narrow stripe of *dpp* mRNA synthesis can be imaged, we constructed a set of singly labeled probes against *dpp* mRNA and performed FISH on imaginal wing discs isolated from third instar larvae while simultaneously performing immunofluorescence against Engrailed protein. We detected *dpp* mRNA in a stripe along the boundary of Engrailed protein expression (**Fig. 3d**,**e**), demonstrating both that the method can be used in wing imaginal discs and that the method can be easily combined with immunofluorescence detection.

Additional tests of our method showed that it was also applicable to *Saccharomyces cerevisae* and cultured rat hippocampal neurons, showing expected specificity in salt-induced expression of the *STL1* gene and dendritic localization of β-actin and *MAP2* mRNAs (**Supplementary Fig. 7** online).

Here we described a FISH method that allows for multiplex gene-expression profiling of transcripts across many model organisms. By using large numbers of singly labeled probes, our method generates uniform signals that can be computationally identified to yield accurate mRNA counts. In contrast, methods using heavily labeled probes (such as dendrimers) can suffer from false positives and negatives owing to individual probe misbinding or nonbinding events, respectively. Another advantage is the simplicity of probe generation and purification; by pooling, coupling and purifying the probes *en masse*, much of the complexity of probe preparation can be avoided. We created a web-based program for designing probe sets with optimally uniform G+C content (http://www.singlemoleculefish.com/). The simplicity of our method will likely facilitate genomic-scale studies of mRNA number and localization with applications in systems biology, cell biology, neurobiology and developmental biology.

Note: Supplementary information is available on the Nature Methods website.

ACKNOWLEDGMENTS

We thank S.A.E. Marras, F.R. Kramer, D. Vargas, S. Sinha, E. Andersen, G. Neuert and Q. Yang. This work was supported by the US National Institute of Mental Health grant MH079197; National Institute of General Medicine grants GM068957, GM077183 and GM070357; and National Science Foundation grant PHY0548484. A.R. is supported by a National Science Foundation fellowship DMS-0603392 and a Burroughs Wellcome Fund Career Award at the Scientific Interface.

Published online at http://www.nature.com/naturemethods/
Reprints and permissions information is available online at http://npg.nature.com/reprintsandpermissions/

1. Kaufmann, B.B. & van Oudenaarden, A. *Curr. Opin. Genet. Dev.* **17**, 107–112 (2007).
2. St. Johnston, D. *Nat. Rev. Mol. Cell Biol.* **6**, 363–375 (2005).
3. Gall, J.G. *Proc. Natl. Acad. Sci. USA* **60**, 553–560 (1968).
4. Levsky, J.M. & Singer, R.H. *J. Cell Sci.* **116**, 2833–2838 (2003).
5. Raap, A.K. *et al. Hum. Mol. Genet.* **4**, 529–534 (1995).
6. Femino, A.M., Fay, F.S., Fogarty, K. & Singer, R.H. *Science* **280**, 585–590 (1998).
7. Maamar, H., Raj, A. & Dubnau, D. *Science* **317**, 526–529 (2007).
8. Femino, A.M., Fogarty, K., Lifshitz, L.M., Carrington, W. & Singer, R.H. *Methods Enzymol.* **361**, 245–304 (2003).
9. Randolph, J.B. & Waggoner, A.S. *Nucleic Acids Res.* **25**, 2923–2929 (1997).
10. Vargas, D.Y., Raj, A., Marras, S.A., Kramer, F.R. & Tyagi, S. *Proc. Natl. Acad. Sci. USA* **102**, 17008–17013 (2005).
11. Raj, A., Peskin, C.S., Tranchina, D., Vargas, D.Y. & Tyagi, S. *PLoS Biol.* **4**, e309 (2006).
12. Wang, J.C. *et al. Proc. Natl. Acad. Sci. USA* **101**, 15603–15608 (2004).
13. Fukushige, T., Hawkins, M.G. & McGhee, J.D. *Dev. Biol.* **198**, 286–302 (1998).
14. Sanicola, M., Sekelsky, J., Elson, S. & Gelbart, W.M. *Genetics* **139**, 745–756 (1995).

nature | methods

Imaging individual mRNA molecules using multiple singly labeled probes

Arjun Raj, Patrick van den Bogaard, Scott A Rifkin, Alexander van Oudenaarden & Sanjay Tyagi

Supplementary figures and text:

Supplementary Figure 1	Computational identification of mRNA spots.
Supplementary Figure 2	Intensity analysis of colocalized spots.
Supplementary Figure 3	Sensitivity of method when using different numbers of probes.
Supplementary Figure 4	Comparison with the mRNA detection method of Femino et al.
Supplementary Figure 5	Examination of fluorescent spot bleedthrough.
Supplementary Figure 6	Demonstration that the oxygen-scavenger increases photostability of Cy5.
Supplementary Figure 7	Imaging single mRNA molecules in yeast and neurons.
Supplementary Methods	

Note: Supplementary Software is available on the Nature Methods website.

Supplementary Figure 1

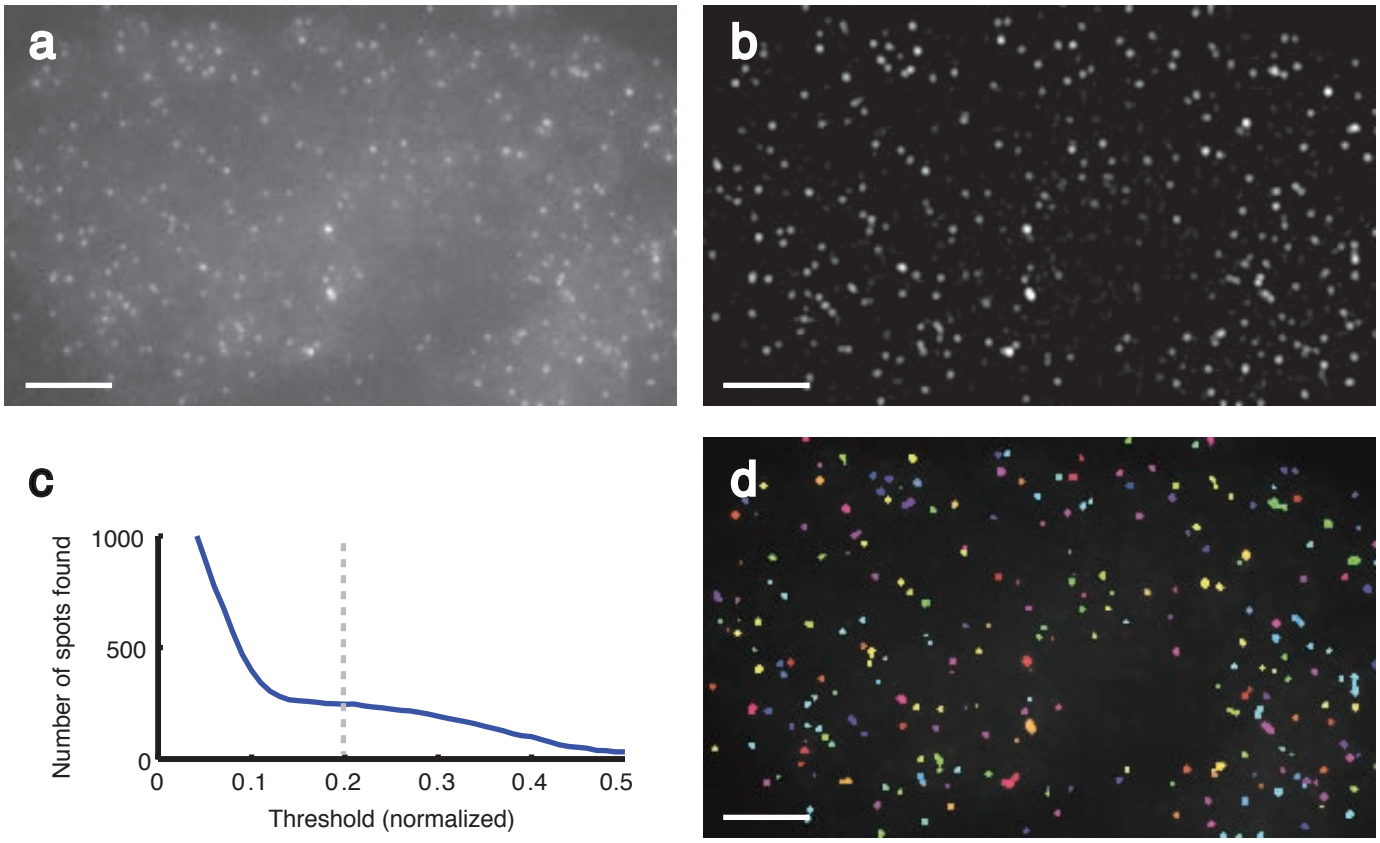

Supplementary Figure 1 | Computational identification of mRNA spots. (**a**) Raw image data (maximum intensity merge) obtained from imaging *FKBP5* mRNA particles in A549 cells induced with dexamethasone. (**b**) Image (maximum merge) obtained by running raw data through Laplacian of a Gaussian filter designed to enhance spots of the correct size and shape while removing the slowly varying background. (**c**) The number of spots (i.e., connected components) found upon thresholding the filtered image from (**b**) is plotted as a function of the threshold value, ranging from 0 to the maximum intensity of the filtered image (normalized to 1). The presence of a plateau indicates that there is a region over which the number of particles detected is fairly insensitive to the particular threshold chosen. The grey line represents the threshold used (within the plateau) for determining the actual number of mRNA in the image. (**d**) Image showing the results of using the threshold represented by the grey line in (**c**) on the filtered image in (**b**), with each distinct spot assigned a random color. The spots detected correspond very well with those identified by eye. All scale bars are 5 μm long.

Supplementary Figure 2

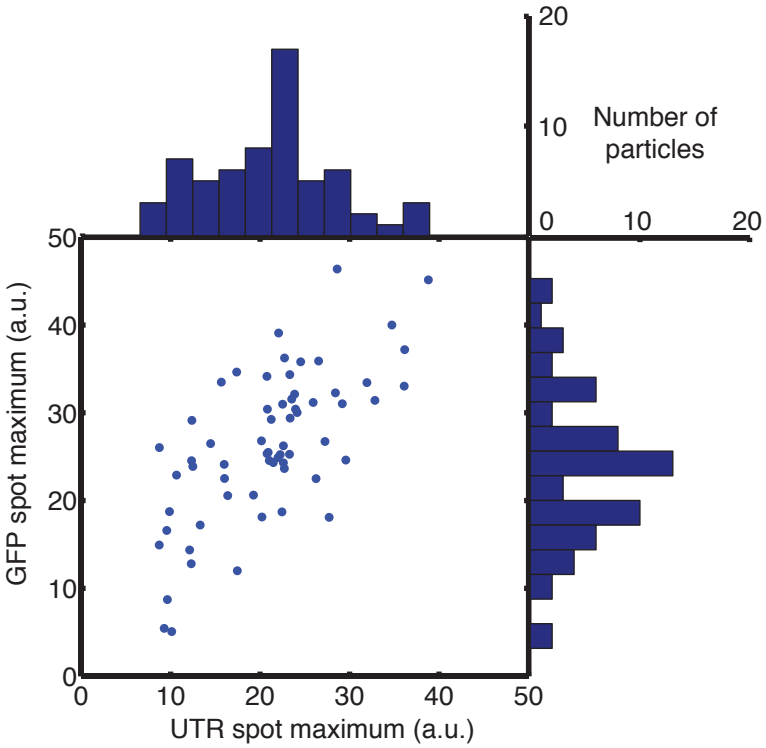

Supplementary Figure 2 | Intensity analysis of colocalized spots. Spot intensities corresponding to the GFP-targeted probes (Alexa 594 channel, y axis) and multimeric UTR-targeted probes (TMR channel, x axis) were computed by taking the maximum intensity in the computationally identified spot region and subtracting the mean intensity of an annular region surrounding the spot. Marginal histograms show the distributions of GFP spot intensities (right) and UTR spot intensities (top).

Supplementary Figure 3

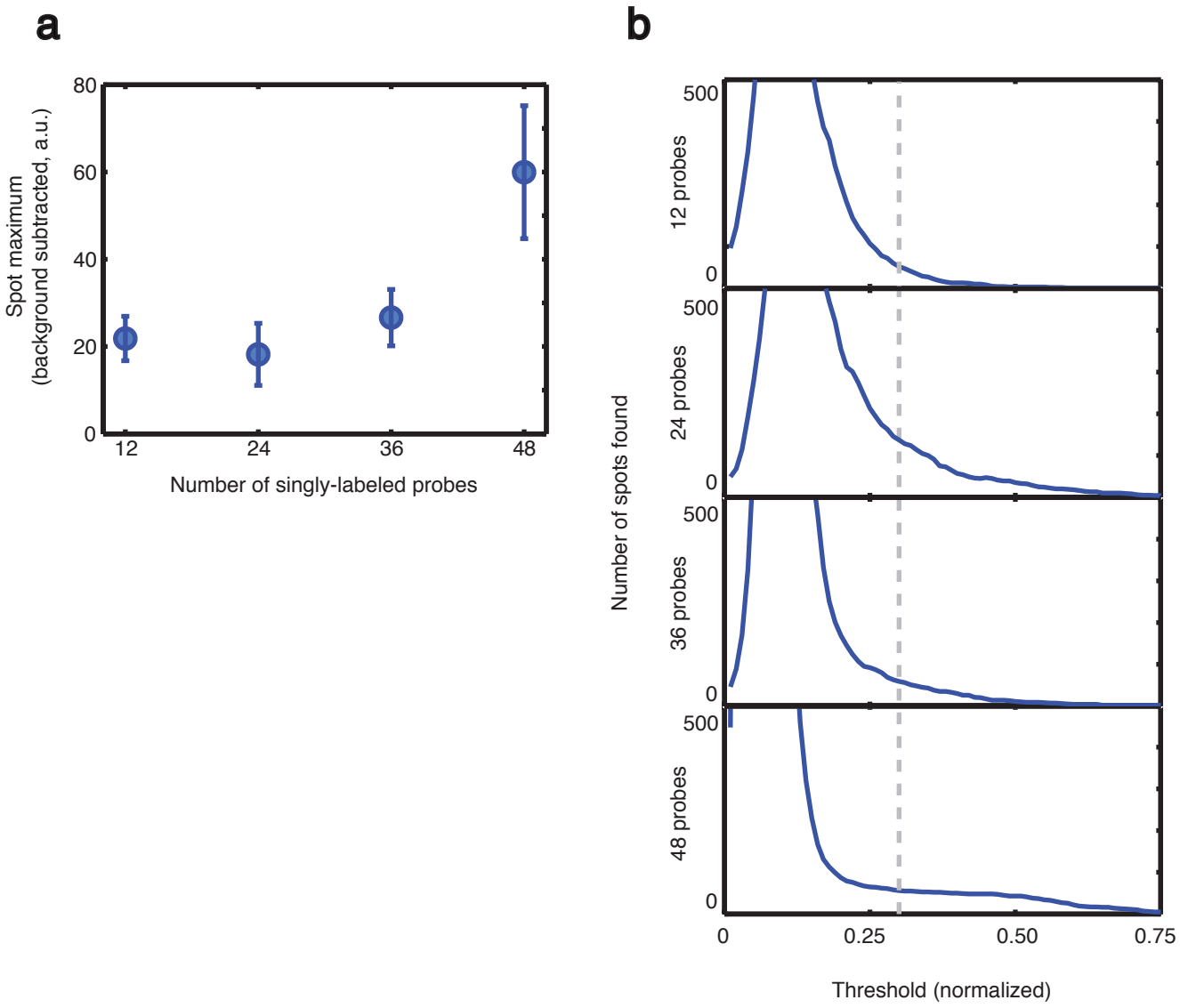

Supplementary Figure 3 | Sensitivity of method when using different numbers of probes. (**a**) Spot intensity (defined as maximum intensity within the spot minus the mean background taken in an annular region surrounding the spot) as a function of the number of probes chosen. Intensities for 12 and 24 probes are artifactual in that spots were not readily identifiable in those cases, so spots identified were biased towards being brighter. (**b**) The number of spots (i.e., connected components) found upon thresholding the filtered image plotted as a function of the threshold value, ranging from 0 to the maximum intensity of the filtered image (normalized to 1) for different numbers of probes. The grey bar indicates the threshold used for the analysis in (**a**).

Supplementary Figure 4

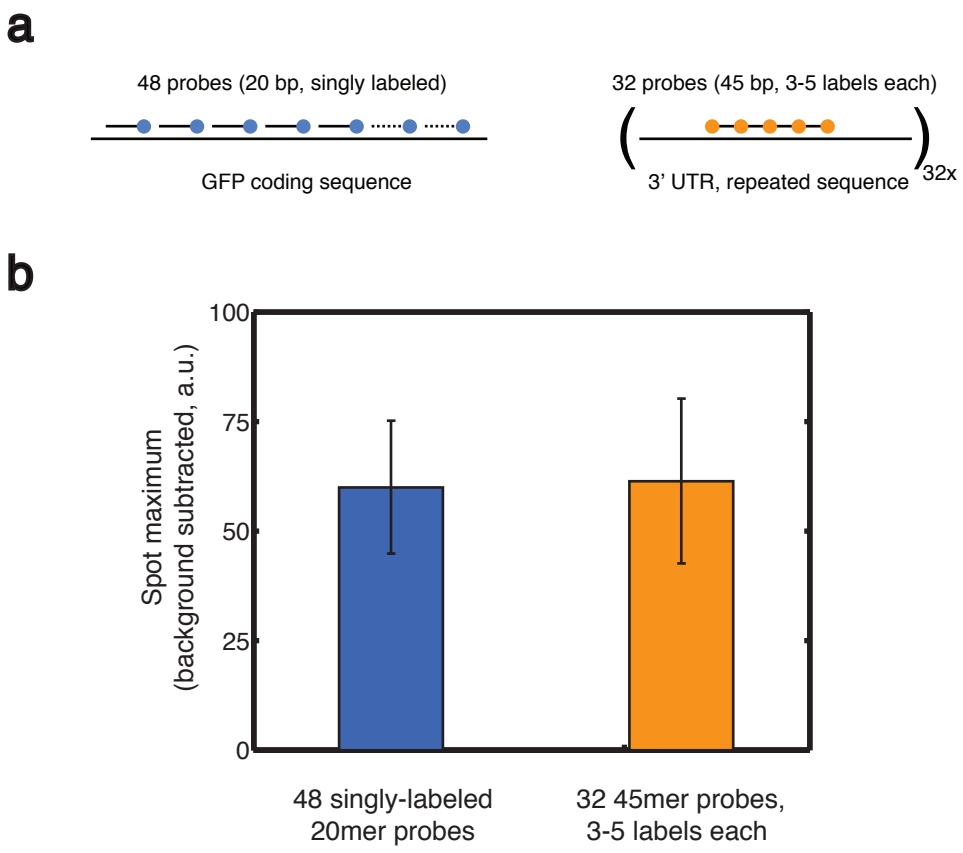

Supplementary Figure 4 | Comparison with the mRNA detection method of Femino et al. (*Science* 1998). (**a**) Schematic depicting the method described in this manuscript with 48 singly-labeled probes (left) and the method of Femino et al. in which each 45 bp probe contains five fluorophores each and is targeted to a sequence element that is repeated 32 times in the 3'UTR of the target mRNA expressed from a transgene in Chinese hamster ovary cells. (**b**) Comparison of spot intensities when using 48 singly labeled probes or using a 45 bp probe labeled with five fluorophores. Error bars represent one standard deviation.

Supplementary Figure 5

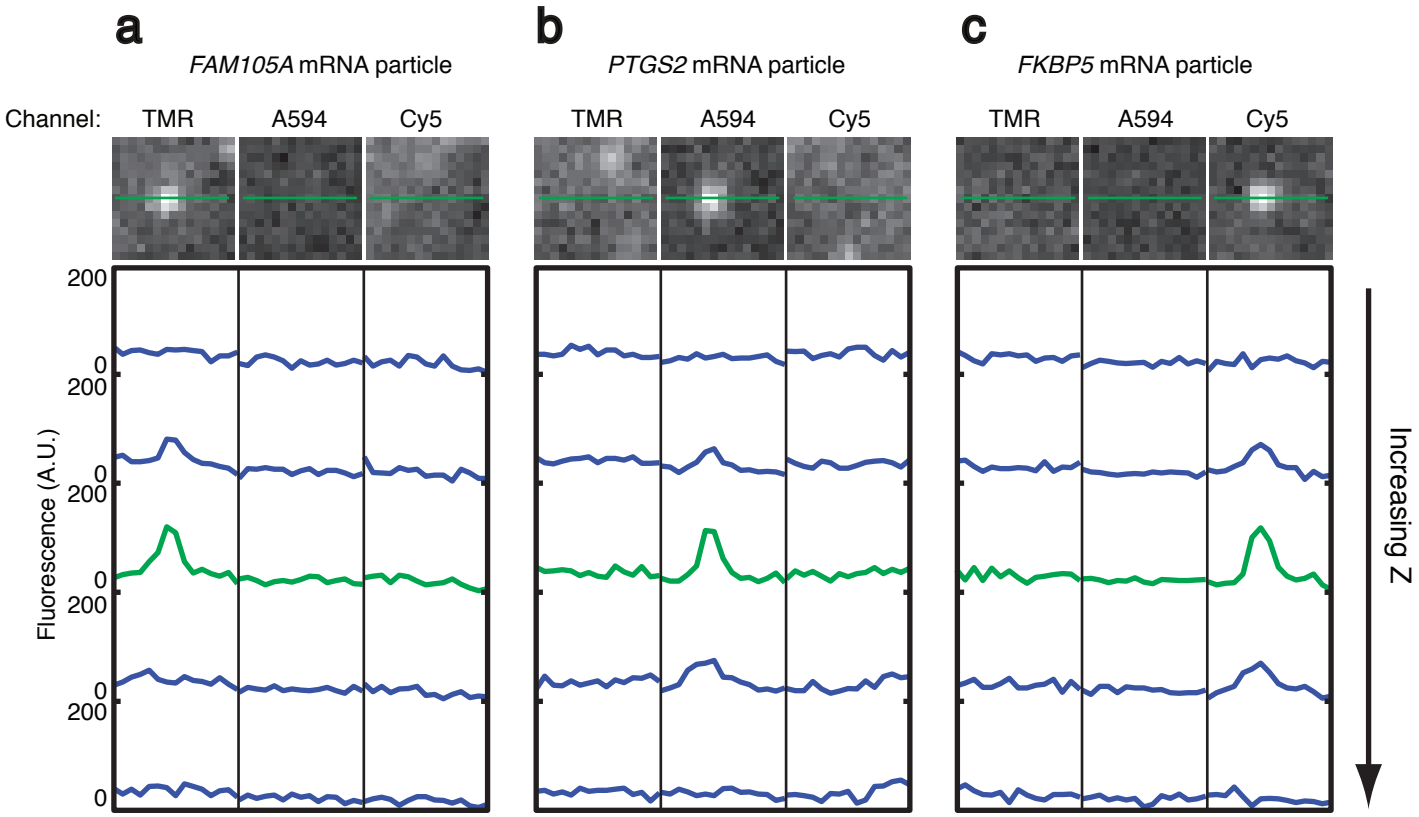

Supplementary Figure 5 | Examination of fluorescent spot bleedthrough. (**a**) Images of an *FAM105A* mRNA spot labeled with TMR as seen through the TMR, Alexa 594 and Cy5 filter channels. Linescans of fluorescent intensity corresponding to the line through the image are given below, with the different linescans corresponding to measurements taken at increasing z (0.25 μm spacing). The green linescan corresponds to the z-slice shown in the image itself. A similar analysis was performed for a *PTGS2* mRNA spot labeled with Alexa 594 (**b**) and an *FKBP5* mRNA particle labeled with Cy5 (**c**). All linescan intensity measurements had the camera background subtracted but range between 0 and 200 arbitrary fluorescence units.

Supplementary Figure 6

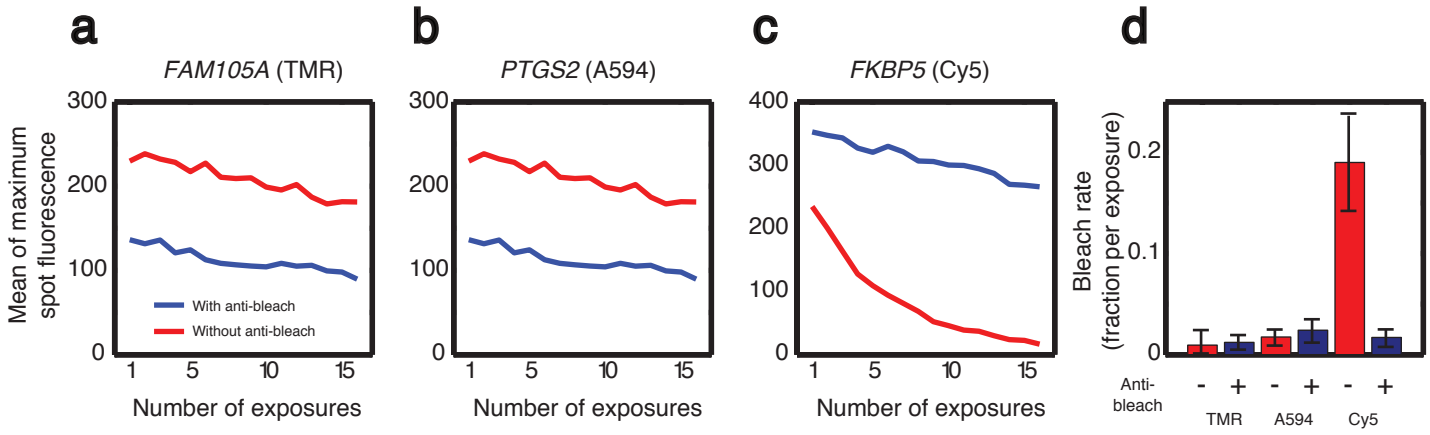

Supplementary Figure 6 | Demonstration that the oxygen-scavenger increases photostability of Cy5. (**a**) The mean of the maximum spot fluorescence for a number of *FAM105A* mRNAs labeled using TMR conjugated probes was plotted as a function of the number of 2 second exposures using a filter specific for TMR. Curves were generated for images taken both with (blue) and without (red) the oxygen scavenging system. A similar analysis was performed for *PTGS2* mRNAs labeled using Alexa 594 conjugated probes with 2 second exposures (**b**) and *FKBP5* mRNAs labeled using Cy5 conjugated probes with 2.5 second exposures (**c**). (**d**) The bleach rate per exposure (in units of fraction of fluorescence lost per exposure) for the TMR, Alexa 594 and Cy5 conjugates probes in (**a**-**c**) both with and without the oxygen-scavenging anti-bleach system. The bleach rate was calculated by fitting each individual particle's decay curve to an exponential and taking the mean of the fitted decay constants. The error bars correspond to one standard deviation. A minimum of 6 particles were chosen in each condition.

Figure overview: One technical challenge that arose when imaging multiple mRNAs simultaneously was fluorophore photolability, particularly in the case of Cy5. In order to image all of the mRNA molecules within a single cell, we acquire 10 to 30 "z-section" images for each visual field, utilizing a one-to-three second exposure for each image and a high numerical aperture objective. Only TMR and (to a lesser extent) Alexa 594 could withstand this intense and relatively prolonged exposure to light; Cy5, for instance, proved extremely photolabile under these conditions. To overcome this problem, we employed a special mounting medium in which fluorophores are much more photostable. This method was adapted from Yildiz et al.[1] with minor modifications. In this medium, a mixture of catalase, glucose oxidase, and glucose enzymatically removes molecular oxygen from the medium, thereby inhibiting oxygen-dependent, light-initiated pathways that destroy fluorophores. The use of these enzymes lead to a dramatic 10-fold enhancement of Cy5 photostability while not adversely affecting the imaging of TMR and Alexa 594, thus facilitating the acquisition of multiple z-sections when performing three color imaging.

1. Yildiz, A. et al. Myosin V walks hand-over-hand: single fluorophore imaging with 1.5-nm localization. *Science* **300**, 2061-2065 (2003).

Supplementary Figure 7

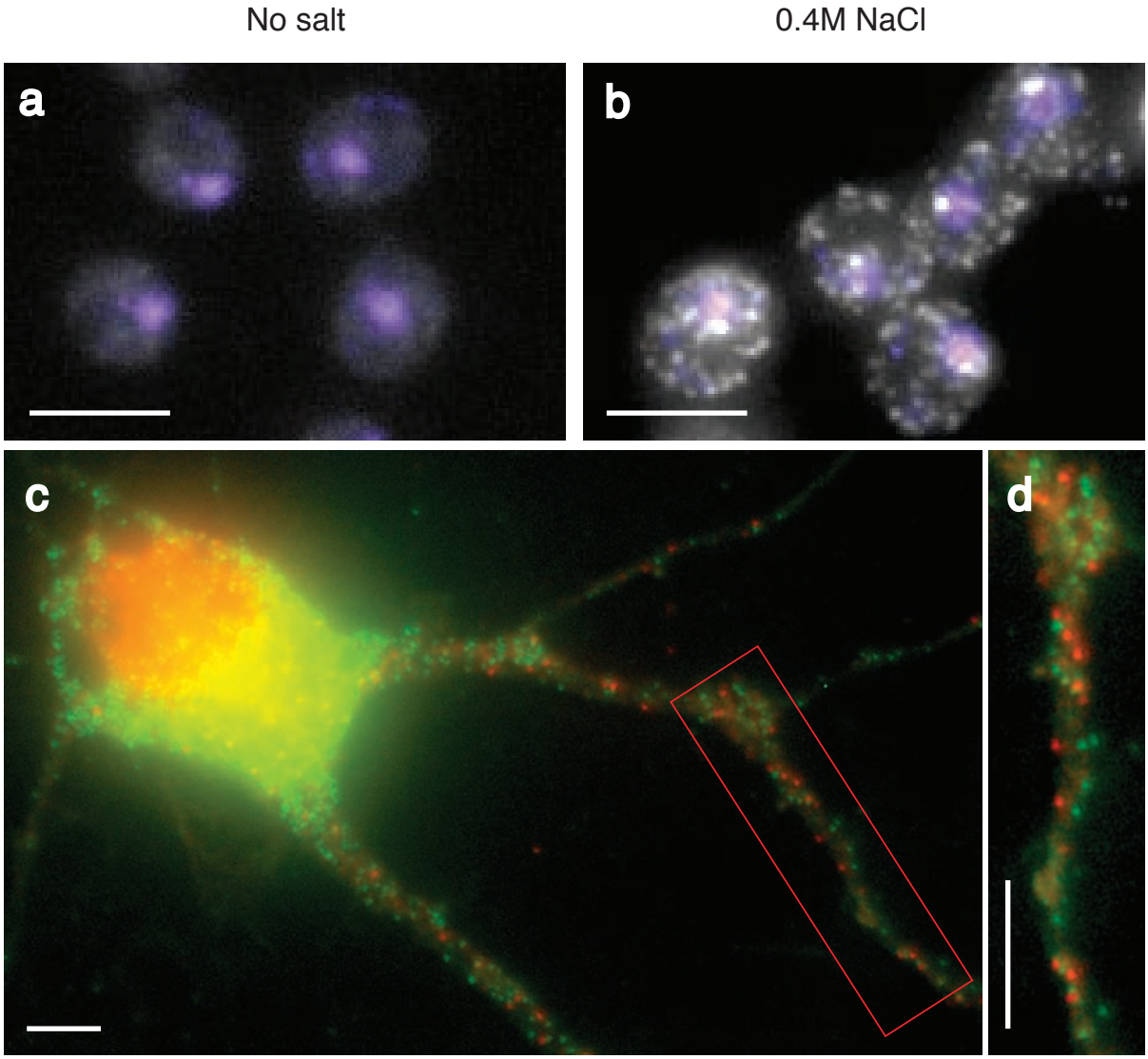

Supplementary Figure 7 | Imaging single mRNA molecules in yeast and neurons. (**a**) *STL1* mRNA particles in both unperturbed cells and (**b**) cells subjected to a 10 minute 0.4M NaCl salt shock, with nuclear DAPI counterstaining in purple. *STL1* is one among a number of yeast genes whose expression is significantly upregulated by the addition of salt to the growth medium[1]. (**c**) Expression of *Actb* (green) and *Mtap2* (red) mRNAs in rat hippocampus neurons in a dissociated neuron culture. (**d**) Enlarged and contrasted image of a segment of a dendrite enclosed by the red box in (**c**). Particle counts indicated that 15% of the 791 *Actb* mRNA molecules were located in dendrites, whereas 37% of the 140 *Mtap2* mRNA molecules were located in the dendrites, similar to previously reported distributions[2,3]. All scale bars are 5 μm long.

References:

1. Rep, M., Krantz, M., Thevelein, J.M. & Hohmann, S. The transcriptional response of Saccharomyces cerevisiae to osmotic shock. Hot1p and Msn2p/Msn4p are required for the induction of subsets of high osmolarity glycerol pathway-dependent genes. *J Biol Chem* **275**, 8290-8300 (2000).

2. Tiruchinapalli, D.M. et al. Activity-dependent trafficking and dynamic localization of zipcode binding protein 1 and beta-actin mRNA in dendrites and spines of hippocampal neurons. *J Neurosci* **23**, 3251-3261 (2003).

3. Blichenberg, A. et al. Identification of a cis-acting dendritic targeting element in MAP2 mRNAs. *J Neurosci* **19**, 8818-8829 (1999).

Supplementary Methods

Synthesis of the probes

The probes were chosen with the following criteria: 1) they should be roughly 17-22 bases long, 2) their GC content should be as close to 45% as possible and 3) there should at least three nucleotides of space between their target regions. To design large number of probes satisfying these conditions, we wrote a program using dynamic programming that optimizes the GC content of each probe subject to the constraints just outlined. This program is available for use on the internet at

http://www.singlemoleculefish.com

A listing of all the probes used in this study aligned with their target mRNA sequence is given at the end of this document (not all probes were designed using the algorithm just described). The oligonucleotides were ordered with 3'-amino modifications from BioSearch Technologies (Novato, California, United States) in plate format with the concentration of each oligonucleotide normalized to 100 μM in water. To couple the oligonucleotides to the appropriate fluorophore, 10 μl were taken from each oligonucleotide, pooled, precipitated and then resuspended in 0.1 M sodium bicarbonate (pH 8.5) with an excess of fluorophore. The fluorophores used were succinomydyl ester derivatives of tetramethylrhodamine (TMR), Alexa-594 (Invitrogen, Carlsbad, California, United States) and Cy5 (Amersham Bioscience, Pittsburgh, Pennsylvania, United States). The coupling proceeded overnight at 37˚C. The excess fluorophore was then removed by ethanol precipitation and then the uncoupled oligonucleotides were separated from the coupled oligonucleotides by reverse phase high pressure liquid chromatography. The coupled fractions were then air-dried in a Speedvac and resuspended in Tris-EDTA, pH 8.0. For each probe, the appropriate concentration for in situ hybridization was determined empirically and was typically around 5-50 ng per hybridization reaction consisting of 50 or 100 μl of hybridization solution.

For the experiments in which different numbers of probes targeting the GFP open reading frame were used, we coupled and purified the first 12, 24, 36 and 48 probes from the set described at the end of this document (*d2EGFP*).

We also generated a probe similar to those used in Femino et al.[1]. The probe sequence was

5′ CGGCRGGTAAGGGRTTCCATARAAACTCCTRAGGCCACGA 3′

where R represents locations where an amino-dT was introduced in place of a regular dT during synthesis; an additional amine group was added by synthesizing the oligo using a controlled pore glass column (Glen Research) that added this group to the 3' end. The probes were coupled to TMR and purified to obtain the most heavily labeled oligonucleotides. Estimates of labeling efficiency show that anywhere between 3 and 5 of the amine groups should be labeled. The construction of the mRNA UTR sequence that this gene targeted was outlined in Raj et al.[2] (designated the M1 multimer).

Mammalian Cell culture

A549 cells (American Type Culture Collection, Manassas, Virginia, United States) were grown on 2-well Lab-tek chambered coverglasses (Nalgene Nunc, Rochester, New York, United States) coated with 0.1% gelatin in DMEM supplemented with L-glutamine, penicillin/streptomycin and 10% Characterized Fetal Bovine Serum (HyClone, Thermo Fisher Scientific, Logan, Utah, United States). The cells were induced for 24 hours through the addition of medium containing 24 nM dexamethasone (Sigma, St. Louis, Missouri, United States). CHO cells were cultured on plain glass coverslips coated with gelatin and placed in culture dishes.

Hippocampus neurons isolated from prenatal Day 18 rats (Brainbits, Springfield, Illinois, United States) were cultured for two weeks on glass coverslips coated with poly-D-lysine and laminin using neurobasal medium (Invitrogen) supplemented with 2% B27 and 0.5% L-glutamine.

Cells attached to chambered coverglass or plain coverslips were fixed by first removing the medium, washing them with PBS buffer (100 mM Na_2HPO_4, 20 mM KH_2PO_4, 137 mM NaCl, 27 mM KCl, pH 7.4), and then incubating them in a solution of PBS with 3.7% formaldehyde for 10 minutes. After the formaldehyde fixation, the cells were washed twice with PBS, permeabilized in 70% ethanol for at least two hours, and then used immediately or stored at 4˚C.

Yeast culture

The yeast strain we utilized was BY4741; Mat a; his3D1; leu2D0; met15D0; ura3D0; YER118c::kanMX4. This strain was grown to an optical density of 0.56 in a 50 mL volume of complete supplemental media without histidine or uracil. The cells were then shocked osmotically by replacing the media with medium containing 0.4M NaCl for 10 minutes. Both shocked and unshocked cells were fixed by adding 5 ml of 37% formaldehyde directly to the medium for 45 minutes. The rest of the fixation and spheroplasting followed the procedure outlined in Long et al.[3] with the following important exception: after spheroplasting, the cells were incubated in concanavalain A (0.1mg/mL, Sigma) for approximately 2 hours before letting them settle onto chambered coverglasses coated overnight with concanavalin A. This increased the efficiency of attachment of the yeast as compared to the more traditional approach of coating the slides with poly-L-lysine.

Worm culture and embryo harvest

The N2 strain of *Caenorhabditis elegans* was grown on plates seeded with OP50 *E. coli* in the standard manner. To extract the embryos from gravid adult hermaphrodites, the worms were washed off the plates in M9 buffer, spun down, and resuspended in a bleaching solution and vigorously shaken for around 5 minutes, at which point the worm bodies themselves are dissolved and only the embryos with their tough chitinous eggshell remain. These embryos were then washed twice with distilled water and then incubated in 1 ml of PBS with 3.7% formaldehyde for 15 minutes. The embryos were then flash frozen by submersion of the tube into liquid nitrogen for 1 minute to crack the eggshells, after which the samples were thawed and incubated for an additional 20 minutes on ice. After that, the embryos were washed twice in PBS and then permeabilized in 70% ethanol for at least 24 hours at 4˚C.

For hybridization with the L1 worm larvae, worms were grown in a mixed stage population as above, washed in PBS, and then resuspended in 1mL of PBS, 3.7% formaldehyde for 45 minutes. After the fixation, the worms were washed twice in PBS and then permeabilized in 70% ethanol for at least 24 hours at 4˚C.

Fly culture and wing imaginal disc harvest

The y cn bw sp strain of *Drosophila melanogaster* was grown according to standard methods. Third instar larvae were isolated and wing discs were manually located and dissected away from the rest of the organism in PBS. The wing discs were placed onto a chambered coverglass and fixed by adding 1 mL of PBS with 3.7% formaldehyde to the chamber for 45 minutes; the fixative was removed by two washes in PBS followed by permeabilization in 70% ethanol for 24 hours at 4˚C.

Fluorescence *in situ* hybridization and imaging

Cells adhered to plain or chambered coverglasses were first rehydrated in a solution of 10% formamide and 2x SSC for 5 minutes. Thereafter, hybridization reactions were performed in 50 µl of hybridization solution containing 10% dextran sulfate, 2 mM vanadyl-ribonucleoside complex, 0.02% RNAse-free BSA, 50 µg E.coli tRNA, 2x SSC, 10% formamide and an empirically determined amount of probe cocktail (typically around 5-50 ng) for 3-24 hours at 37˚C (Singer lab protocol). For the cells attached to chambered coverglass, a coverslip was placed over the hybridization solution both to spread the small volume over the entire surface of the chamber and to prevent evaporation during the overnight incubation. The hybridization reactions with cells grown on plain coverslips were performed by placing them over a drop of hybridization solution on a flat piece of parafilm.

After hybridization the cells were washed twice for 30 minutes at 30˚C using a wash buffer (usually 10%, 15% or 20% formamide and 2xSSC). Nuclear staining was performed by adding DAPI (Invitrogen) to the wash solution during the second wash. For TMR and Alexa-594 labels the imaging was performed using either PBS or 2xSSC as mounting medium. When the Cy5 dye was used as the label, or when we employed long exposure times for imaging with other fluorophores, we used freshly prepared oxygen depleted mounting media. We prepared 100 µl aliquots of this medium just before use by adding 1µl of 3.7mg/mL glucose oxidase and 1µl of catalase suspension (both from Sigma, St.Louis, Missouri, United States) to 10 mM Tris HCl pH 8.0, 2xSSC, and 0.4% glucose, a modification of the system developed by Yildiz et al.[4]. The plain coverslips were mounted on glass slides and sealed with clear nail-polish and chambered coverglasses were covered with a coverslip to prevent evaporation and any influx of oxygen during imaging.

The C. elegans embryos and worms were hybridized in solution. For hybridization, the samples were first spun down using a swinging bucket centrifuge, after which the 70% ethanol was aspirated and the samples were resuspended in a solution of 10% formamide and 2xSSC for 5 minutes. The samples were then spun down again and the supernatant was aspirated. Then 100µl of hybridization solution containing 10% formamide was added to the sample and incubated overnight at 30˚C. The next day, the samples were washed twice by adding 1 ml of wash solution consisting of 10% formamide and 2xSSC, spinning and aspirating the supernatant, and then adding

another 1 ml of wash solution and incubating the samples for 30 minutes at 30˚C. These two washes were followed by another wash and incubation in the same solution supplemented with 5 µg/ml DAPI. Finally the samples were allowed to settle to the bottom of a chambered coverglass and imaged.

For the fly wing discs, immunofluorescence was incorporated into the FISH protocol in the following manner. During the overnight hybridization, the 55 µl of hybridization solution (with 10% formamide) was supplemented with 1 µl of mouse anti-Engrailed antibody (4D9 anti-engrailed/invected-s, Developmental Studies Hybridoma Bank at the University of Iowa) in addition to the probe mixture for *dpp* mRNA detection. In the morning, the samples were washed 2x in 10% formamide, 2xSSC for 30 minutes at 30C. Afterwards, another 55 µl of hybridization solution with 10% formamide supplemented with 1 µl of Alexa-488 goat anti-mouse secondary antibody (Invitrogen) was added to the sample and covered with a cover slip. The secondary labeling proceeded for 1 hour after which the sample was washed twice with 10% formamide, 2xSSC for 30 minutes at 30˚C. Finally, the samples were kept in 2xSSC for imaging.

The images for the colocalization analysis and the images for the neurons were taken with a Zeiss Axiovert 200M inverted fluorescence microscope (Zeiss, Oberkochen, Germany) equipped with a 100x oil-immersion objective and a CoolSNAP HQ camera (Photometrics, Pleasanton, California, United States) using Openlab acquisition software (Improvision, Sheffield, United Kingdom). All other images were taken with a Nikon TE2000 inverted fluorescence microscope equipped with a 100x oil-immersion objective and a Princeton Instruments camera using MetaMorph software (Molecular Devices, Downington, Pennsylvania, United States). Custom narrow band filters to discriminate between TMR and Alexa 594 were obtained from Omega Optical (Brattleboro, Vermont, United States) and broad band filters for TMR, Alexa 594 and Cy5 was obtained from Chroma (Rockingham, Vermont, United States). Typical exposure times used were 1 second for the broad band filters for TMR and Alexa 594 and 3 seconds for the narrow band filters and for the Cy5 filter. Stacks of images were taken automatically with 0.25 microns between the *z*-slices.

Measurements of bleaching rate

A549 cells were grown in 2 chambers of chambered coverglass and induced overnight with medium containing 24nM dexamethasone. After we performed fixation, hybridization and washing as outlined above, we added 2xSSC to one of the chambers and added the anti-bleach solution described above to the other chamber. To measure the rate of photobleaching, we repeatedly imaged spots using 2.5 second exposures for Cy5 and 2 second exposures for TMR and Alexa 594. We then computationally identified spots as described below and measured their maximum intensity as a function of the number of exposures taken. We then computed the average photobleach rate for each spot individually by fitting the intensity profile to an exponential; the average of this value was taken to be the rate of photobleaching.

Measurements of spot intensities using different numbers of probes

A549 cells were grown in 2 chambers of chambered coverglass and induced overnight with medium containing 24nM dexamethasone. After we performed fixation, hybridization and washing as outlined above, we added 2xSSC to one of the chambers

and added the anti-bleach solution described above to the other chamber. To measure the rate of photobleaching, we repeatedly imaged spots using 2.5 second exposures for Cy5 and 2 second exposures for TMR and Alexa 594. We then computationally identified spots as described below and measured their maximum intensity as a function of the number of exposures taken. We then computed the average photobleach rate for each spot individually by fitting the intensity profile to an exponential; the average of this value was taken to be the rate of photobleaching.

Image analysis and particle identification

In order to identify and locate particles in a semi-automated way, images were processed using custom software written in MATLAB (The Mathworks, Natick, Massachusetts, United States).. The first step was to apply a linear filter roughly corresponding to a Laplacian convolved with a Gaussian to remove the non-uniform background while enhancing particles. The optimal bandwidth of the filter (corresponding to the width of the Gaussian) depends on the size of the observed particle and was empirically adjusted to maximize the signal to background of the particles. While this filter enhances particulate signal, noise still appears in the filtered image, necessitating the use of a threshold. The choice of threshold is an important step in accurate determination of mRNA particle number. To perform this in a principled manner, we counted the number of spots for all possible thresholds, where a spot was defined as a connected component in three dimensions. Upon plotting the number of spots detected as a function of the threshold, we typically observed a plateau corresponding to a range of thresholds over which the number of mRNAs detected did not vary. The existence of this plateau indicates that the particle signals are easily detected above background. Moreover, thresholds chosen in this region yielded spot detection that matched very nicely with spots identified by eye. In some cases (typically those with very high background), a plateau did not appear but was rather replaced by a "kink" in the graph. Choosing a threshold at the location of the kink yielded mRNA spot detection that corresponded closely with manual identification. Overall, it was difficult to computationally identify the region where the plateau was without some human guidance, so our method is only semi-automated, but with graphical aides, hundreds of thresholds can be chosen an hour due to the robust appearance of the plateaus. Generally, our algorithm was run on a cell-by-cell basis, thus removing potential differences in signal to background level in different cells in the same field.

For the colocalization analysis, we looked for thresholded particle voxels that overlapped in the two channels; such particles were considered to be colocalized. Software, including all the custom filters used, is available upon request.

For particle intensity measurements, we would first identify the particles as described and take the maximum intensity within the connected component that defines the spot. From this value, we subtracted the local background by taking the mean intensity of an annular region surrounding the spot. We used maximum intensities rather than mean intensities because the use of mean or total intensities is heavily dependent on the size of the spot, which is not a mathematically well-defined quantity and can lead to artifacts in the analysis.

RT-PCR analysis of *FKBP5* induction

A549 cells were grown in 8 chambers of chambered coverglass, of which 4 were induced with medium containing 24nM dexamethasone while the 4 others were grown in medium without dexamethasone. After 8 hours of induction, one of the chambers each from both the induced and uninduced batches was fixed as outlined above while the cells in the remaining 3 chambers were harvested for RT-PCR using the RNeasy Mini Kit (Qiagen, Valencia, California, United States). The RNA was extracted by removing the medium and washing once with PBS, after which 300µl of the cell lysis buffer was added directly to each chamber and mixed by pipetting as per the protocol accompanying the kit, after which the protocol was followed to completion, resulting in three independent RNA isolations each for both the induced and uninduced cells.

The RT-PCRs were performed using the one-step QuantiFast SYBR Green RT-PCR kit (Qiagen) using 5 µl of a 1:10 dilution of template RNA in a 25µl reaction with the following primers (5' to 3'):

FKBP5:	ATTGTCAAAAGAGTGGGGAATG	(forward)
	GCCAAGACTAAAGACAAATGG	(reverse)
PTGS2:	GTCAAAACCGAGGTGTATGT	(forward)
	ATAATTGCATTTCGAAGGAA	(reverse)
FAM105A:	GGACATTGTTAAGCTTCCTG	(forward)
	TTCAGTCCACTGTGTTTTCA	(reverse)

RT-PCRs on each of the three independent isolations were done in triplicate, resulting in 9 measurements for both the uninduced and induced samples. A standard curve was generated by performing RT-PCR on 5µl of 1:1, 1:10, 1:100 and 1:1000 dilutions of one of the induced samples. The variability in the threshold cycles for the uninduced and induced samples was used to compute the error for the RT-PCR fold induction as follows: the standard error was computed for both uninduced and induced threshold cycles and error bars were determined by computing the fold induction for the mean threshold cycle with the standard errors added and subtracted in such a manner as to maximize the error.

In parallel, we performed in situ hybridization on the fixed sample and obtained stacks of fluorescence images for 53 uninduced and 57 induced cells. These images were then analyzed as above to obtain the number of *FKBP5*, *PTGS2* and *FAM105A* mRNAs per cell. Errors in the fold induction as determined by in situ hybridization were obtained by bootstrapping 1000 averages of both the induced and uninduced populations and then finding the standard deviation of the fold induction of the bootstrapped means.

References

1. Femino, A.M., Fay, F.S., Fogarty, K. & Singer, R.H. Visualization of single RNA transcripts in situ. *Science* **280**, 585-590 (1998).
2. Raj, A., Peskin, C.S., Tranchina, D., Vargas, D.Y. & Tyagi, S. Stochastic mRNA synthesis in mammalian cells. *PLoS Biol* **4**, e309 (2006).
3. Long, R.M., Elliott, D.J., Stutz, F., Rosbash, M., Singer, R.H. Spatial consequences of defective processing of specific yeast mRNAs revealed by fluorescent in situ hybridization. *RNA* 1(10), 1071-1078 (1995)
4. Yildiz, A. et al. Myosin V walks hand-over-hand: single fluorophore imaging with 1.5-nm localization. *Science* **300**, 2061-2065 (2003).